Enhanced Quantum Dot Emission of Multimode Photonic Crystal Nanocavities

Mohang G. Olemwang, Mohammad A. Ahmad*

Department of Electronic Engineering, Faculty of Engineering, Central University of Diourbel, Diourbel, SENEGAL
Email: mohammedahmed1964@yahoo.com

Abstract
This letter explores the design, fabrication and characterization of multimode photonic crystal cavities to support the emission of quantum dots via the Purcell effect. The results showed the existence of three optical resonant modes with high quality factors (~10^3) as well as achievement of different field distributions to match the positions of quantum dots. Despite that the experimental values of Purcell factor were lower than 5 – compared to theoretical values reaching 100 – the proposed design was successful in light trapping and producing strong resonance. This work shows the possibility to use these multimode cavities to support the control of emission and applications of integrated photonic quantum circuits.

Keywords: Quantum dots; Photoluminescence; Resonance modes; Multimode cavities
Received: December 2025; **Revised:** January 2026; **Accepted:** February 2026; **Published:** April 2026

1. Introduction

Nanobeam photonic crystal cavities are one of the most promising platforms in the field of quantum information due to their super capability to confine light within ultra-small sizes near the wavelength scale. This leads to exceptionally support the light-matter interaction. The designs of these cavities depend on the construction photonic bandgap throughout a periodic pattern of holes in a nanowaire. This allows to trap the optical modes inside the central defect region. The maximum significance of these structures show an ability to achieve high quality Q-factor accompanied by very small mode size to allow the appearance of Purcell effect. Theoretically, Purcell factor (F_P) is defined as the measure of the acceleration of the spontaneous emission rate of the light source inside the cavity compared to the free space. It is expressed mathematically as:

$$F_P = \frac{3}{4\pi^2}\left(\frac{\lambda}{n}\right)^3 \frac{Q}{V_{eff}} \quad (1)$$

where λ is the wavelength, and n is the refractive index

The transformation from monomode to multimode systems presents new tool to simultaneous control the emissions at different frequencies. This supports the design flexibility in the applications requiring complex quantum correlation or ultra-accurate sensing.

The semiconducting quantum dots – mostly referred to as artificial atoms – are considered as the ideal partner of radiation nano-cavities due to their narrow emission lines and high efficiencies as single-photon emitters. When such quantum dots are incorporated into a multimode cavity, it is possible to adjust the energy levels of the quantum dots to match one of the cavity modes. This leads to support the Purcell enhancement and guide the emitted photons with high efficiency towards a critical output situation. Current research works aim to invest the multimode feature to overcome the conventional restrictions of the frequency bandwidth. Such cavities allow strong coupling or weak coupling with the multiple energy levels of quantum dots, and then enhance the purity of single photons and indistinguishability.

The deep understanding of theoretical concepts relating the classical electromagnetism and quantum dynamics inside such cavities can be considered as the key to improve integrated quantum photonic circuits with ability to operate at high efficiency as the mode engineering plays a crucial role in decreasing the light loss, and increasing the emitter-cavity coupling rate.

2. Experimental Part

GaAs photonic crystal cavities based on multimode nanobeams were designed, fabricated and characterized to support the emission of quantum dots (QDs) via the Purcell effect as the high optical cavity is maintained. The experimental work was started by determining the engineering standards to keep the quantum dots far from the grooved edges at a distance not smaller than 300 nm to avoid the spectral broadening resulted from the surface defects. These structures were fabricated on a radially-grown wafer containing a 190nm GaAs layer and InAs QDs with density higher than 1 /μm^2 over a layer of AlGaAs.

The fabrication process was performed by electron beam lithography and inductively-coupled reactive plasma ionic lithography to translate the nanomodes to the GaAs layer. Then the AlGaAs layer was removed by HF treatment to produce hollow structures. In order to characterize the performance, an imaging setup for micro-photoluminescence (PL) at very low temperature (1.8K) while the device is excited with a 780nm laser source.

Measurements showed the presence of three apparent optical resonance modes to agree with the simulation expectations and Q-factor of about 10^3. The radiative decay measurements were carried out to 11 single quantum dots coupled to these cavities using ultra-sensitive photonic detectors. Despite that the theoretical expectations refer to the possibility of achieving Purcell factor up to 100, the experimental findings showed values lower than 5, and this difference is attributed to the excitonic dynamics and the temperature of slow carriers resulted from the nonresonant excitation, in addition to the random distribution of QDs positions. A numerical simulation confirmed that these factors limit the ability to track larger modifications under the conditions of the current experiment.

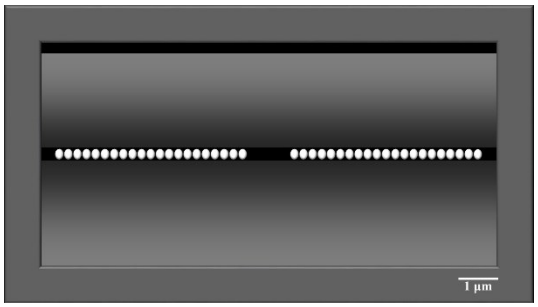

Fig. (1) A microscopic image of the photonic crystal cavities based on multimode nanobeams fabricated in this work

3. Results and Discussion

Figure (2) shows the spatial distribution of the transverse electric field component (TEM_{00}, TEM_{01}, and TEM_{02}) incorporated in a multimode GaAs nanobeam waveguide. The dimensions of this waveguide are maintained at 750nm width and 400nm thickness at wavelength of 940nm. These dimensions represent the practical model fabricated and discussed in this work. In the TEM_{00} mode, the field intensity distribution is concentrated at the center of the structure away from the edges, which makes it ideal to achieve strong match to the uantum dots at the center. The TEM_{01} mode shows that the field distribution splits into two longitudinal parts with a node at the center. The TEM_{02} mode shows three transversely-distributed parts of field intensity.

These modes are significantly important in designing photonic crystal nanocavities as they – according to the proposed simulation – contribute to the formation of optical resonances (M5, M6, and M7). For instance, the M7 resonance reasonably depends on the components of the fundamental mode (TEM_{00}), while the M5 and M6 resonances represent the field beating resulted from higher order modes like TEM_{02}. The use of a 750nm-width waveguide is intended strategy to ensure that the quantum dots are far enough from the side walls of the groove. This reduces the spectral broadening resulted from charge fluctuations on the surfaces. The formation of multimodes increases the design complexity when compared to the single-mode waveguides, however, these spatial distributions allow higher flexibility for resonant excitation of quantum dots throughout the higher-ordered modes while quality factors up to 10^3 and small mode sizes are sufficiently maintained to provide reasonable increase in the spontaneous emission rate (Purcell effect) exceeding 100 in the ideal situations.

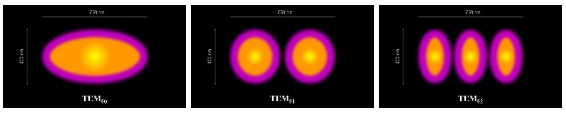

Fig. (2) Spatial distributions of transverse-electric (TE) modes of multimode nanobeam waveguide (750nm width and 400nm thickness) at 940nm wavelength

Figure (3) shows the photoluminescence (PL) spectra recorded for the three different photonic GaAs crystal cavities designed using the multimode nanobeam waveguides. These spectra were produced by ensemble InAs quantum dots at the center of GaAs layer using a powerful nonresonant excitation laser with 940nm wavelength at low temperature. These spectra clearly show three resonant sharp peaks for each device, classified according to the theoretical modeling of M5, M6, and M7 modes as these peaks lie within the emission range of the quantum dots of 900-1050nm). The possible variations in the geometry and refractive index were considered according to the finite-element modeling (FEM). Based on these spectra, the increase in the minimum lattice parameter (a_m) from 160 to 180 nm leads to an apparent redshift in the resonant peaks for all modes, which completely agrees with the physical concepts of the photonic cavities where the resonance wavelength increase with geometrical dimensions. The experimentally-measured quality factors (Q) of these peaks differ as the M7 mode shows the maximum PL intensity at a_m=170nm as all values were in the theoretically-expected range (10^3).

Appearance of sharp peaks in the emission background of the quantum dots confirms that the design is successful in light trapping and generating strong optical resonances despite the complex multimode nature of the waveguide. The matching between measured and simulated peaks refers to the

accurate fabrication using electron-beam lithography and ionic reactive grooving. These spectra can be considered as an optical fingerprint allowing researchers to determine the modes for later coupling with the single quantum dots to study the Purcell effect. While the strong nonresonant excitation shows an excellent cavity response, it is shown that study of accurate radiative decay requires different excitation conditions to overcome the bottle-neck phonon effects and carrier relaxation dynamics, which may not be apparently observed in continuous PL spectra but affect the lifetime measurements.

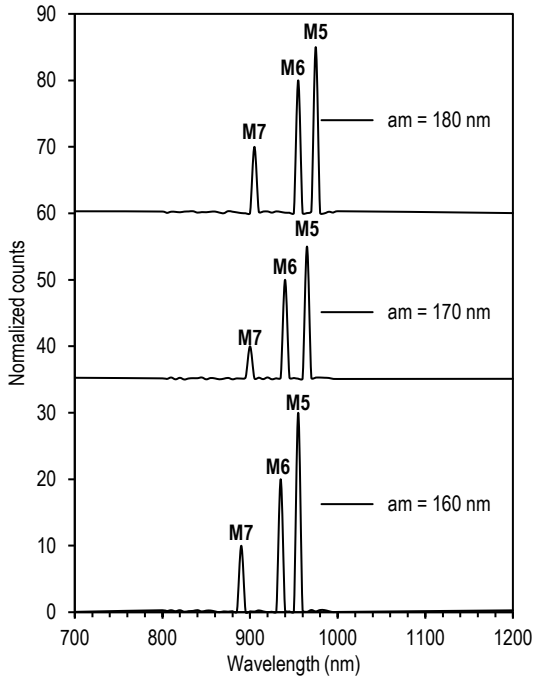

Fig. (3) Measured PL spectra produced by QDs ensemble under strong nonresonant optical excitation for multimode nanobeam cavities

4. Conclusion

In concluding remarks, the designed and fabricated multimode photonic GaAs crystal cavities can efficiently trap the light and produce featured optical resonant modes with quality factors up to 10^3, which support the light-matter interaction. Despite that the measured Purcell factor values were lower than 5, the proposed design confirmed its ability to match the field modes with the positions of quantum dots and narrowed spectral broadening. Results highlight the practical limitations, such as excitonic dynamics and random dot distribution, with the capability of such multimode devices to develop integrated photonic quantum circuits with much more complexity and flexibility.

References

[1] M. Barhoumi, R. Bassoli and F.H.P. Fitzek, "Quantum qubit-optical cavity node: Effects of the temperature and coupling strengths on the cavity Fock-state distribution occupation probability and entropy of the subsystems using Dicke model", *Result Phys.*, 72 (2025) 108214.

[2] S. Castelletto et al., "Deterministic placement of ultra-bright near-infrared color centers in arrays of silicon carbide micropillars", *Beilstein J. Nanotech.*, 10 (2019) 2383-2395.

[3] M. Giglio et al., "Broadband detection of methane and nitrous oxide using a distributed-feedback quantum cascade laser array and quartz-enhanced photoacoustic sensing", *Photoacoust.*, 17 (2020) 100159.

[4] M. Giaquinto, "Stimuli-responsive materials for smart Lab-on-Fiber optrodes", *Result Opt.*, 2 (2021) 100051.

[5] M. Pan et al., "Polarization-insensitive narrowband reflective wavefront manipulation through all-dielectric anisotropic subwavelength structures", *iScience*, 28(4) (2025) 112147.

[6] M.A. Khan et al., "Hybrid plasmonic coupling through multilayer optimum microcavity based quantum dots random laser", *J. Lumines.*, 287 (2025) 121455.

[7] J. Zhu and J. Lou, "High-sensitivity Fano resonance temperature sensor in MIM waveguides coupled with a polydimethylsiloxane-sealed semi-square ring resonator", *Result Phys.*, 18 (2020) 103183.

[8] R.-R. Meng et al., "Solid-state quantum nodes based on color centers and rare-earth ions coupled with fiber Fabry–Pérot microcavities", *Chip*, 3(1) (2024) 100081.

[9] F.D. Santillan and A. Hanke, "Rabi oscillations and entanglement between two atoms interacting by the Rydberg blockade studied by the Jaynes–Cummings Model", *Phys. Open*, 24 (2025) 100292.

[10] S. Weigl et al., "Photoacoustic detection of acetone in N_2 and synthetic air using a high power UV LED", *Sens. Actuat. B: Chem.*, 316 (2020) 128109.

[11] F. Pilat et al., "Hot-cavity linewidth enhancement factor of a quantum cascade laser", *Opt. Laser Technol.*, 182(B) (2025) 112112.

[12] M. Cahay and S. Bandyopadhyay, "Semiconductor Quantum Devices", P.W. Hawkes (ed.), **Advances in Electronics and Electron Physics**, Academic Press, Vol. 89 (1994), pp. 93-253.

[13] T. Jennewein et al., "QEYSSat 2.0—white paper on satellite-based quantum communication missions in Canada", *Canad. J. Phys.*, 103(4) (2024) 328-376.

[14] U. Zamir et al., "Intracavity laser absorption spectroscopy: Performance and advantages for energy science", *Appl. Energy Combus. Sci.*, 17 (2024).

[15] D.-R. Li et al., "Single nanowire integrated microfiber devices", *Result Opt.*, 5 (2021) 100199.

[16] O. Melchert et al., "Two-color soliton meta-atoms and molecules", *Optik*, 280 (2023) 170772.

[17] P. Hautle and W.Th. Wenckebach, "Creating high, portable proton polarization with photo-excited triplet DNP", *J. Mag. Resonance Open*, 20 (2024) 100159.

[18] K. Beltrán et al., "Subthreshold and reverse bias model of graphene/p-type silicon Schottky diodes", *J. Sci.: Adv. Mater. Dev.*, 10(3) (2025) 100925.

[19] S. Shahid, S.-E. Zumrat and M.A. Talukder, "A merged lattice metal nanohole array based dual-mode plasmonic laser with an ultra-low threshold", *Nanoscale Adv.*, 4(3) (2022) 801-813.
[20] S. Mikki, "Theory and computation of Markovian quantum antenna systems", *Result Phys.*, 49 (2023) 106453.
[21] G. Heinrich et al., "Dynamics of coupled multimode and hybrid optomechanical systems", *Comptes Rendus Physique*, 12(9-10) (2011) 837-847.
[22] E. Desurvire et al., "Science and technology challenges in XXIst century optical communications", *Comptes Rendus Physique*, 12(4) (2011) 387-416.
[23] K. Singh et al., "Cathodoluminescence as a probe of the optical properties of resonant apertures in a metallic film", *Beilstein J. Nanotech.*, 9 (2018) 1491-1500.
[24] A. ur Rehman et al., "A comparative study of the photonic crystals-based cavities and usage in all-optical-amplification phenomenon", *Photon. Nanostruct. Fundam. Appl.*, 61 (2024) 101298.
[25] S. Berneschi et al., "From laboratory to prototype: the last-mile issue in whispering gallery mode resonator-based devices", *Opt. Mater.*, 167 (2025) 117248.
[26] M. Schmidt et al., "Dynamic beam shaping—Improving laser materials processing via feature synchronous energy coupling", *CIRP Annals*, 73(2) (2024) 533-559.
[27] G.H.M. van Tartwijk and G.P. Agrawal, "Laser instabilities: a modern perspective", *Prog. Quantum Electron.*, 22(2) (1998) 43-122.
[28] J. Wekalao et al., "Machine learning-driven terahertz graphene-MXene-gold metasurface biosensor for dual COVID-19 and cervical cancer biomarker detection", *Sens. Bio-Sens. Res.*, 50 (2025) 100920.

